0022-3565/99/2893-1391$03.00/0
THE JOURNAL OF PHARMACOLOGY AND EXPERIMENTAL THERAPEUTICS
Copyright © 1999 by The American Society for Pharmacology and Experimental Therapeutics
JPET 289:1391–1397, 1999

Vol. 289, No. 3
Printed in U.S.A.

Pharmacological Properties of Trimebutine and *N*-Monodesmethyltrimebutine

FRANCOIS J. ROMAN, SANDRINE LANET, JACQUES HAMON, GILLES BRUNELLE, ANNE MAURIN, PASCAL CHAMPEROUX, SERGE RICHARD, NICOLE ALESSANDRI, and MAURICE GOLA

Institut de Recherche Jouveinal/Parke Davis, Fresnes Cedex, France (F.J.R., S.L., J.H., G.B.); Centre de Recherches Biologiques, Chemin de Montifault, Baugy, France (A.M., P.C., S.R.); and Laboratoire de Neurobiologie, Unité Propre de Recherche, Centre National de la Recherche Scientifique, Marseille Cedex, France (N.A., M.G.)

Accepted for publication February 1, 1999 This paper is available online at http://www.jpet.org

ABSTRACT

Trimebutine [2-dimethylamino-2-phenylbutyl-3,4,5-trimethoxybenzoate hydrogen maleate (TMB)] has been demonstrated to be active for relieving abdominal pain in humans. To better understand its mechanism of action, we have tested TMB; nor-TMB, its main metabolite in humans; and their respective stereoisomers for their affinity toward sodium channels labeled by [^{3}H]batrachotoxin, their effect on sodium, potassium, and calcium currents in rat dorsal root ganglia neurons, and their effect on veratridine-induced glutamate release from rat spinal cord slices. TMB has also been tested in an animal model of local anesthesia. TMB (K_i = 2.66 ± 0.15 μM) and nor-TMB (K_i = 0.73 ± 0.02 μM) displaced [^{3}H]batrachotoxin from its binding site with affinities similar to that of bupivacaine (K_i = 7.1 ± 0.9 μM). nor-TMB was found to block veratridine-induced glutamate release with an IC_{50} value of 8.5 μM, which is very similar to that of bupivacaine (IC_{50} = 8.2 μM); the effect of TMB was limited to 50% inhibition at 100 μM. TMB and nor-TMB blocked sodium currents in sensory neurons from rat dorsal root ganglia (IC_{50} = 0.83 ± 0.09 and 1.23 ± 0.19 μM, respectively), whereas no effect was observed on calcium currents at the same concentrations. A limited effect was observed on potassium currents (IC_{50} = 23 ± 6 at 10 μM) for TMB. In vivo, when tested in the rabbit corneal reflex, TMB displayed a local anesthetic activity 17-fold more potent than that of lidocaine.

Trimebutine (TMB) has been used in many countries since 1969 for the treatment of functional bowel disorders, including irritable bowel syndrome (IBS). The efficacy of the compound to relieve abdominal pain has been demonstrated in various clinical studies using different protocols of treatment (Moshal and Herron, 1979, Lüttecke, 1980; Toussaint et al., 1981; Ghidini et al., 1986). The activity of the compound was first believed to be due to its spasmolytic activities as in the case of phloroglucinol, mebeverine, or pinaverium. However, as distinct from the antispasmodic compounds, TMB was found to display weak agonist activity for rat brain and guinea pig (Roman et al., 1987) or canine (Allescher et al., 1991) intestinal opioid receptors, without selectivity for any of the μ, δ, and κ subtypes. This weak activity was confirmed when using isolated intestinal fragments under transmural stimulation (Pascaud et al., 1987). This property could be responsible for the modulatory action of TMB on intestinal motility in fasted dog. TMB given either i.v. or orally delays the appearance of phase III of the migrating motor complex in the stomach and the duodenum by inducing a premature phase III, migrating along the whole intestine (Bueno et al., 1987). In humans, TMB stimulates intestinal motility in both fed and fasted states (Grandjouan et al.,1989). Furthermore, TMB reverses the effect of stress in jejunal motility (Delis et al., 1994).

More recently, TMB has been shown able to influence the activity of visceral afferents by decreasing the intensity of the rectocolonic reflex in rats as demonstrated by the inhibition of colonic motility consecutive to rectal distention (Julia et al., 1996). This result may be related to the beneficial effects found with TMB in patients with IBS and, more specifically, in the treatment of attacks of abdominal pain. To better understand the mechanism of action underlying the efficacy of TMB in visceral pain, we investigated the effect of TMB on sodium channel currents, on veratridine-induced glutamate release from rat spinal cord slices, and in a model of local anesthesia.

Because pharmacokinetic studies in humans have shown that when given orally TMB is metabolized in liver to give nor-TMB, the main metabolite of TMB, which reaches plasma levels higher than those of TMB itself. We have also included in this study nor-TMB, as well as the stereoisomers of TMB [(*R*)-TMB and (*S*)-TMB] and of nor-TMB [(*R*)-nor-TMB and (*S*)-nor-TMB].

Received for publication September 23, 1998.

ABBREVIATIONS: NMDA, *N*-methyl-D-aspartate; IBS, irritable bowel syndrome; TMB, trimebutine.

Materials and Methods

Animals

Male Sprague-Dawley rats (IFFA Credo, Saint Germain sur l'Arbresle, France), weighing 225 to 250 g ([^{3}H]batrachotoxin-binding experiments) or 350 to 375 g (glutamate-release experiments), or pregnant rats (electrophysiological experiments) were used in this experiment and were cared for in accordance with the institutional guidelines for animal welfare (temperature, 21 ± 3°C; light/dark, 12 h/12 h).

Male New-Zealand White rabbits (CEGAV; Les Hauts Noës, Saint Mars d'Egrenne, France) weighing 1.9 to 2.7 kg were used. Animals were housed individually in cages placed in an air-conditioned (17–21°C) animal house kept between 45% and 65% relative humidity and with an artificial day/night cycle (12 h/12 h) with lights on at 7.30 AM

Drugs and Media

TMB, (*S*)-TMB, (*R*)-TMB, nor-TMB, (*S*)-nor-TMB, and (*R*)-nor-TMB were synthesized by Sipsy (Avrillé, France). Flunarizine, L-glutamatic acid, lidocaine hydrochloride, bupivacaine, trypsin, and Dulbecco's modified Eagle's medium/Ham's F-12 were purchased from Sigma (St. Quentin Fallavier, France). Morphine was from Francopia (Gentilly, France). Veratridine was from RBI, Bioblock Scientific (Illkirch, France). Gentamicin was from Boehringer Mannheim S.A. (Meylan, France). All reagents used for the preparation of buffers and solutions were of analytical grade from Merck-Clevenot (Nogent sur Marne, France).

L-[G-^{3}H]Glutamic acid (49 Ci/mmol) was from Amersham (Les Ulis, France). Dulbecco's modified Eagle's medium, Neurobasal medium, and fetal calf serum were from Gibco Life Technologies S.A.R.L. (Cergy Pontoise, France). Horse serum was from Seromed (Berlin, Germany).

[^{3}H]Batrachotoxin Binding

Synaptosomal Membranes. Cerebral cortices from male Sprague-Dawley rats were homogenized in a glass-Teflon homogenizer in 10 volumes of ice-cold 0.32 M sucrose and 5 mM K_2HPO_4, pH 7.4 at 4°C. The homogenate was centrifuged at 1000*g* for 10 min; the new pellet was resuspended in the same volume of sucrose and recentrifuged. The new pellet was discarded, and the two supernatants resulting from these two centrifugations were pooled and centrifuged at 20,000*g* for 10 min. The resulting pellet was resuspended in a sodium-free assay buffer containing 50 mM HEPES, 5.4 mM KCl, 0.8 mM $MgSO_4$, 5.5 mM glucose, and 130 mM choline chloride, pH 7.4 at 25°C.

Binding Experiment. Binding assays were initiated by the addition of 150 to 200 mg synaptosomal protein to an assay buffer containing 25 μg scorpion venom (*Leireus quinquestriatus*), 0.1% BSA, 10 nM [^{3}H]batrachotoxin, and various concentrations of test drugs (250 μl final volume). Nonspecific binding was determined in the presence of 0.3 mM veratridine. Reactions were incubated for 90 min at 25°C, and the bound ligand was separated from the free by vacuum filtration through GF/B filters (Filtermate; Packard). The filters were washed with 2× 5 ml of buffer (5 mM HEPES, 1.8 mM $CaCl_2$, 0.8 mM $MgSO_4$, 130 mM choline chloride, 0.01% BSA; pH 7.4 at 25°C), and bound ligand was estimated by using liquid scintillation spectrometry (Topcount; Packard).

Calculations. In all experiments examining the displacement of [^{3}H]batrachotoxin binding by unlabeled drugs, concentration-response curve were generated using six concentrations of drugs. All assays were performed at least three times, with each determination performed in duplicate. Data are expressed as mean values ± S.E.M. of at least three determinations. Displacement curves were fits generated by GraphPAD Software (San Diego, CA). Displacement plots were analyzed by a nonlinear regression analysis using the LIGAND computer program (McPherson, 1985). These analyses generated Hill coefficient (n_H) and IC_{50} values. K_i values were calculated from IC_{50} values using the Cheng-Prusoff (1973) relationship.

Glutamate Release Experiment

Buffers. Two buffers were prepared: an incorporation buffer (modified Krebs' solution containing 119 mM NaCl, 5 mM KCl, 0.75 mM $CaCl_2$, 1.2 mM $MgSO_4$, 1 mM NaH_2PO_4, 25 mM HEPES, 1 mM $NaHCO_3$, 11 mM D-glucose, 67 μM EDTA, 1.1 mM L-ascorbic acid, pH 7.4, gassed with 95% O_2/5% CO_2) and a superfusion buffer identical to the incorporation buffer except that EDTA and ascorbic acid were omitted. Compounds to be tested and veratridine were diluted in this superfusion buffer.

Rat Spinal Cord Slices. After the decapitation of animals, a 1.5-cm segment of lumbar spinal cord was isolated after a lumbosacral laminectomy and submerged in a ice-cold modified Krebs' solution gassed with 95% O_2/5% CO_2. After removal of the dura matter, all ventral and dorsal roots were cut at the root of the entry zone. Slices (250-μm-thick cube-like blocks) were prepared using three successive sections performed with McIllwain tissue chopper.

Superfusion Experiments. Slices were incubated for 5 min at 30°C in 5 ml of incorporation buffer maintained under oxygenation and containing 10 μM L-glutamic acid and 4 μCi/ml [^{3}H]glutamic acid. After incubation, the slices were transferred into superfusion chambers in an automatic superfusion apparatus (Brandel). The apparatus consisted in a device of 20 chambers, which allowed 20 experiments to run simultaneously and controlled the sequence of buffers used in the superfusion through the programming of an Apple IIe computer. This system made it possible to test various experimental groups in the same run (four groups of five chambers). After a washout period of 45 min, at a flow rate of 0.5 ml/min, veratridine (40 μM) was added for 5 min to the superfusion medium. When drugs were tested, they were added to the superfusion medium 15 min before and also during veratridine application. Fractions of superfusate corresponding to 5 min were collected during the 30-min period after the stimulation. At the end of the run, the slices were removed from the chambers, and 2.5 ml of scintillation liquid (Hionic Fluor; Packard) was added to the slices and to each of the fractions. The radioactivity was determined using liquid scintillation spectroscopy (Minaxi; Packard). The efflux of radioactivity was assumed to be due mainly to [^{3}H]glutamate efflux (Turner and Dunlap, 1995).

Data Analysis. All values were expressed as the mean ± S.E.M. of at least five determinations. Release of radioactivity for each fraction was expressed in terms of fractional release calculated by dividing the radioactivity in each fraction by the amount remaining in the filter. The stimulation produced by veratridine was quantified by cumulating the release of radioactivity measured in the fractions collected after the stimulation. The effect of tested compounds was evaluated as percent of inhibition by comparing the total amounts of radioactivity released in control chambers with those released in chambers superfused with test compounds. From these percent inhibitions, IC_{50} values were calculated by plotting probit values of inhibition versus log values of concentrations. Statistical analyses were performed using Student's unpaired two-tailed *t* test. Statistical differences were considered significant at $P < .05$.

Electrophysiological Experiments

Dorsal Root Ganglia (DRG) Neurons. Experiments on sodium and calcium currents were constructed using cultured rat DRG excised from 14- to 15-day-old rat embryos. Methods for cell isolation and culture were derived from those described by Valmier et al. (1989). Pregnant Sprague-Dawley rats were sacrificed by placing them in a CO_2 atmosphere for 5 to 6 min. Three to five embryos were removed aseptically and placed in a Petri dish containing the following B medium supplemented with antibiotics (50 μg/ml streptomycin and 50 U/ml penicillin). The B medium contained 137 mM NaCl, 5.4 mM KCl, 0.4 mM Na_2HPO_4, 0.8 mM $MgSO_4$, 0.8 mM $MgCl_2$, 1.8 mM $CaCl_2$, 6 mM glucose, and 10 mM HEPES. The DRG were removed

from the excised spinal cord and digested for 6 min in 2 ml of Dulbecco's modified Eagle's medium containing 0.1% trypsin. Cells were dissociated mechanically through fire-polished Pasteur pipettes and plated in polyornithine-laminine-coated dishes. The culture medium was the Neurobasal medium containing 0.5 mM glutamine and 25 μM glutamate. The cells were incubated at 37°C in 5% CO_2. Electrophysiological experiments were performed from 4 to 6 to 24 h after plating.

Rat Pituitary Cell Line GH_3/B_6. This cell line, of rat pituitary origin, exhibits voltage-dependent calcium currents of low and high activation thresholds, as well as tetrodotoxin-sensitive sodium currents (Matteson and Armstong, 1984). Proliferating GH3 cells were grown at 37°C in a 5% CO_2 environment. The growth medium contained Dulbecco's modified Eagle's medium-Ham's F-12 supplemented with 12.5% horse serum and 2.5% fetal calf serum. When the cells came to confluence, they were split and replated at 5×10^4 cells in 5 ml growth medium.

Potassium Channels Expressed in *Xenopus* Oocytes. Two voltage-dependent potassium channels were considered: the shaker-related Kv1.1 and Kv1.2 channels. These channels were selected in view of their involvement in the central and peripheral nervous system, particularly at nerve endings and Ranvier nodes of myelinated fibers (Wang et al., 1994).

The rat voltage-dependent rKv1.1 and rKv1.2 channels were expressed in *Xenopus* oocytes. The rKv1.1 and rKv1.2 cDNAs were a generous gift from S. Alper (Beth Israël Hospital, Havard Medical School, Boston, MA). The transcriptions were performed using the Ambion Megascript (Ambion, Austin, TX), and the cRNAs were stored in water at 1 mg/ml. cRNA injection in *Xenopus* oocytes was done at 2 to 4 ng/ml. Defolliculated oocytes were maintained in ND96 medium supplemented with 0.1 U/ml gentamicin. The currents were recorded 1 to 6 days after injection.

Electrophysiology. Conventional whole-cell patch-clamp experiments were performed at room temperature using an EPC7 (List) patch-clamp amplifier. CH3/B6 cells and DRG neurons were bathed in a Hanks'-derived medium containing 143 mM NaCl, 10 mM $CaCl_2$, 5.6 mM KCl, 2 mM $MgCl_2$, 5 mM glucose, and 10 mM HEPES, pH adjusted to 7.4 with NaOH (osmolarity, 300–310 mOsm/liter). Calcium currents were recorded in the presence of 10^{-5} M tetrodotoxin and 10 mM tetraethylammonium. For recording sodium current, calcium was replaced by Mg^{2+} in the presence of 10 mM tetraethylammonium. Patch electrodes used for recording sodium and calcium currents were filled with saline containing 140 mM CsCl, 1.1 mM EGTA, 5 mM HEPES, and 2 mM $MgCl_2$, pH adjusted to 7.2 to 7.3 with CsOH (osmolarity, 290 mOsm/liter). The electrodes were pulled in four steps from 1.5 mM glass capillaries (GC 150 TF; Clark Electromedical Instruments) using a P87 puller (Sutter Instruments) and fire-polished. The tip resistance was 2 to 3 MΩ.

Drugs were dissolved in the bath medium (from stock solutions at 10^{-2} M in dimethyl sulfoxide) and applied by pressure ejection (Pneumatic Picopump PV820; WPI) from glass pipettes (10–20-μm tip diameter) located 50 to 60 μm from the recorded cell.

A two-electrode voltage-clamp amplifier (Geneclamp 500; Axon Instruments) was used to record potassium currents from *Xenopus* oocytes. The KCl (3 M)-filled electrodes had tip resistance of <1 MΩ. The oocytes were continuously superfused with a calcium-free ND96 medium to abolish the large calcium-activated Cl^- current present in these cells.

Calculations. Data were sampled at 2 kHz. Software for stimulation, acquisition, and analysis was constructed in house. The dose-response curves were constructed with various drug concentrations separated by wash periods. Each point was the mean ± S.E.M. of three to six experiments. Experimental points were fitted to the theoretical Hill curve using the least-squares Minsq program: $y = 1/(1 + [X]^n/IC_{50}{}^n)$, where y is the fraction of sodium current persisting in the presence of the drug applied at the concentration $[X]$, IC_{50} is the concentration of drug that half-blocks the sodium current, and n is the Hill coefficient corresponding to the number of drugs required to block one sodium channel.

Rabbit Corneal Reflex

Corneal Reflex Testing. Test substances were administered as solutions in sterile water (Baxter, Maurepas, France). The concentrations of test substances were expressed as percentage (weight/volume) of active compound (base form). Each test substance at each concentration was tested on the two eyes of five animals (i.e., 10 measurements per substance and per concentration). On the day of the study, animals were placed in restraint cages in a quiet room. Twenty to 30 min later, a first measurement of the corneal sensitivity was performed. Any animal presenting a partial or complete corneal insensitivity or any ocular lesion before administration was excluded from the study. Immediately after the first measurement, 2× 50 μl of test substances or their vehicle was applied to the cornea. The two instillations were undertaken on each eye at a 1-min interval. Corneal sensitivity was subsequently measured at 5, 10, 20, 30, 40, 50, and 60 min after the instillations and then at 2, 3, and 4 h after the instillations. Corneal sensitivity was measured by touching gently the center of the cornea with a loop-shape nylon yarn (0.3-mm diameter). For each measurement, this operation was repeated 10 times at regular 2-s intervals. The number of stimulations producing a corneal reflex was noted for each set and for each eye.

Calculations. Results were expressed as percentage of inhibition of the corneal reflex calculated for each set of 10 stimulations: percent inhibition of corneal reflex = 10 − (number of stimulations inducing a corneal reflex) × 10.

For each experimental group, median values were determined. The effects of test compounds were compared with those of the vehicle using a Mann-Withney nonparametric U test at each time of measurement. Areas under curves were calculated over the first 60-min period after instillation for each animal, and each concentration was calculated by the trapezoidal method of Bourget and Delouis (1993). The relative potency of TMB was compared with that of lidocaine hydrochloride from respective mean areas under curves using ANCOVA.

Results

[^{3}H]Batrachotoxin Binding

TMB, nor-TMB, and their stereoisomers displaced [^{3}H]batrachotoxin from its binding sites to rat cortical synaptosomes with potencies lying between that of bupivacaine (K_i = 7.14 ± 0.96) and that of flunarizine (K_i = 0.38 ± 0.05 μM). For all compounds, the displacement of [^{3}H] batrachotoxin was complete and the calculated Hill coefficient was close to 1 (Fig. 1).The affinity of nor-TMB (K_i = 0.73 ± 0.02 μM) was higher than that of TMB (K_i = 2.66 ± 0.15 μM). For both compounds, no stereoselectivity was evident because the corresponding stereoisomers displayed affinities similar to those of racemates. For TMB, the values for the (*S*)- and (*R*)-enantiomers were K_i = 3.31 ± 0.36 μM and K_i = 2.89 ± 0.88 μM, respectively. For nor-TMB, the values for the (*S*)- and (*R*)-enantiomers were K_i = 0.80 ± 0.04 μM and K_i = 1.26 ± 0.07 μM, respectively.

[^{3}H]Glutamate Release

TMB inhibited dose-dependently veratridine-induced glutamate release, but no significant effect was found at concentrations lower than 60 μM (Fig. 2). Furthermore, no more than 50% to 60% inhibition could be reached at concentrations as high as 100 μM. (*R*)-TMB presented a profile similar to that of the racemate, whereas (*S*)-TMB looked more active, with a significant inhibition being obtained from the concen-

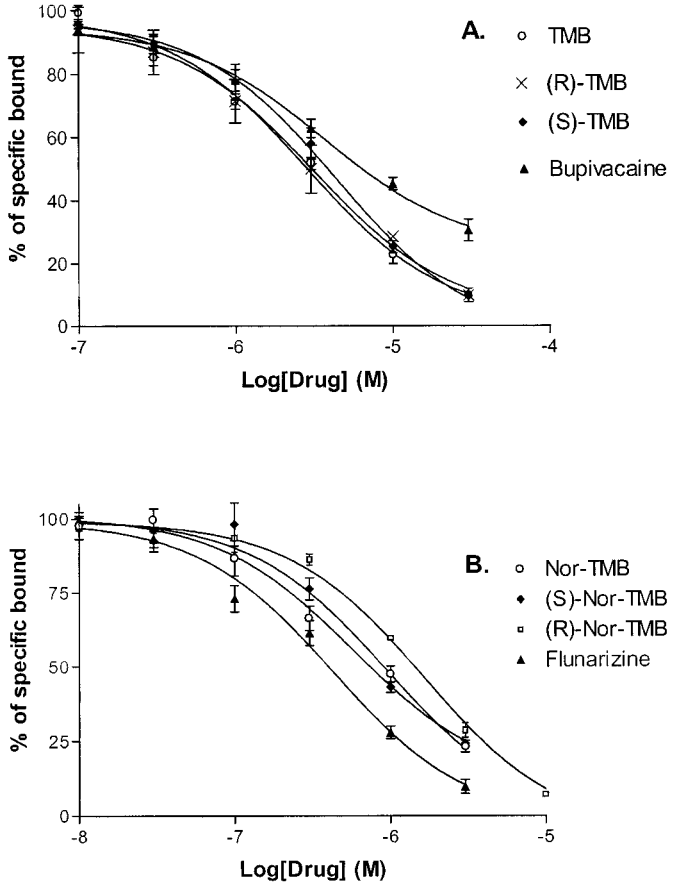

Fig. 1. Effect of TMB (A), nor-TMB (B), and their corresponding stereoisomers on [^{3}H]batrachotoxin binding to rat cortical synaptosomes. Membranes were incubated with increasing concentrations of test drugs in presence of 25 mg scorpion venom and 10 μM [^{3}H]batrachotoxin. Nonspecific binding was determined in the presence of 0.3 mM veratridine. After a 90-min incubation at 25°C, bound ligand was separated from free ligand by vacuum filtration through GF/B filters. Specific binding in presence of test compounds is calculated as percentage of control binding determined in absence of inhibitors. Represented values are mean ± S.E.M. from at least three independent determinations performed in duplicate.

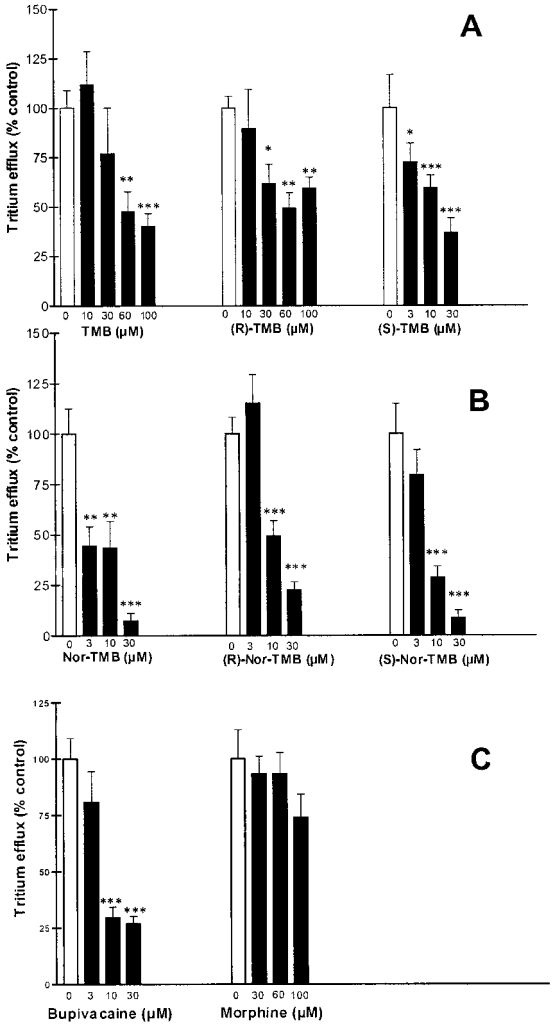

Fig. 2. Effect of TMB (A), nor-TMB (B), and their corresponding stereoisomers on veratridine-induced glutamate release from rat spinal cord slice. Morphine and bupivacaine (C) were tested in the same condition. Results are mean ± S.E.M. of at least 10 determinations. The slices were superfused 15 min with the test compound before stimulation with veratridine (40 μM). The radioactivity collected in 5-min fractions during 30 min after the stimulation was counted, and the effect of compound was determined by comparing the cumulated quantity of radioactivity released with that obtained in cells superfused with buffer alone. *$P < .05$; **$P < .01$;***$P < .001$, Student's t test. Open bars indicate release with buffer alone; filled bars, release in the presence of indicated compounds.

tration of 3 μM. The estimated IC_{50} value was 15.2 μM for (*S*)-TMB, whereas it could not be calculated ($IC_{50} > 100$ μM) for TMB and (*R*)-TMB.

For nor-TMB (Fig. 2B), the inhibitory effect was significant ($p < .01$) at 3, 10, and 30 μM and the IC_{50} value was 8.4 μM. (*S*)-nor-TMB displayed an activity (IC_{50} = 6.3 μM) similar to that of the racemate and similar also to that of the second enantiomer, (*R*)-nor-TMB (IC_{50} = 16.3 μM). When bupivacaine was evaluated under the same experimental conditions, we could estimate an IC_{50} value of 8.2 μM. Morphine was found to be inactive in this paradigm up to 100 μM (Fig. 2C).

Electrophysiological Experiments

Sodium Currents. Figure 3A shows the effects of the successive 20-s applications of TMB at 0.1 and 1 μM on the sodium current of a DRG neuron. In this representative experiment, TMB induced a reversible blockade of the current amounting to 13% and 61% at 0.1 and 1 μM, respectively. The blockade occurred without any evidence of changes in current kinetic (Fig. 3B) and voltage dependence (Fig. 3C). The dose-response curve obtained by applying 0.01, 0.1, 1, and 10 μM TMB is shown in Fig. 3D as a plot of the current part remaining in the presence of the blocker. The inhibition parameters calculated from this curve were IC_{50} = 1.05 ± 0.09 and n_H = 1.09 ± 0.10. The same experiments performed using nor-TMB and (*S*)-nor-TMB led to the following parameters for nor-TMB (IC_{50} = 0.82 ± 0.09 μM, n_H = 1.02 ± 0.07) and for (*S*)-nor-TMB (IC_{50} = 0.69 ± 0.05 μM, n_H = 1.01 ± 0.07). Some experiments performed on the sodium currents of GH3 cells led to very similar results for the three compounds (results not shown).

A kinetic study was performed using (*R*,*S*)-TMB and (*S*)-nor-TMB. The unblocking rate k_{off} was determined from the time constant $\tau_{off} = 34 \pm 4$ s ($n = 6$) of the exponential recovery from block: $k_{off} = 1/\tau_{off} = 29 \cdot 10^{-3} \cdot s^{-1}$. The blocking rate k_{on} was deduced from $K_D = k_{off}/k_{on}$; $k_{on} = 35–40 \cdot 10^{-3} \cdot s^{-1} \cdot \mu M^{-1}$.

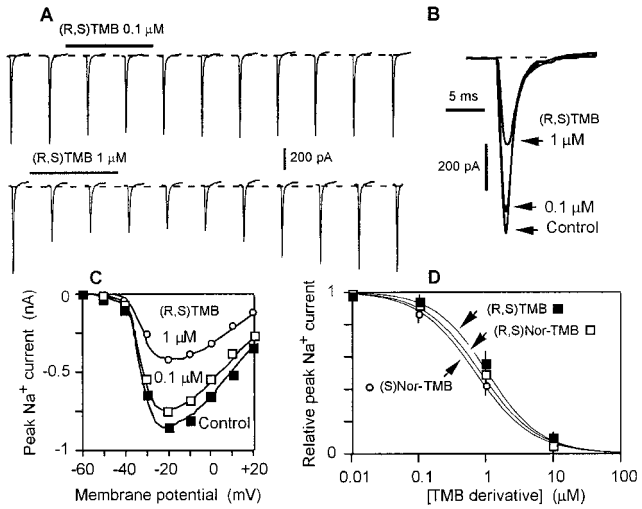

Fig. 3. A, effect of TMB on sodium currents measured in DRG neurons. A, inward sodium current induced every 10 s by stepping the membrane potential from −80 to −10 mV. TMB was locally applied for 20 s at 0.1 μM (top row) and at 1 μM (bottom row). B, sodium current before (control) and during TMB perfusion (same cell as in A). C, peak sodium current versus pulse potential in control saline and in the presence of TMB at the concentrations indicated. The decrease in peak sodium current occurred homothetically. D, dose-response relationship of TMB effects on DRG sodium current. Results are expressed as the sodium current part (relative peak sodium current) persisting in the presence of the blocker. Each point is mean ± S.E.M. of four to six experiments. Continuous curve: best fit to Hill function with IC_{50} = 0.69 μM and n_H = 1.02.

These reaction rates defined the three drugs as fast sodium channel blockers; for instance, 10 μM (*R*,*S*)-TMB blocked the channels with a time constant of 2.2 s.

Calcium Currents. In both GH3 cells and DRG neurons, the three drugs applied at 10 μM had no significant effects on either the low-threshold transient T-type calcium currents (early peak in Fig. 4A) or the high-threshold slowly inactivating calcium currents (steady state inward current in Fig. 4A).

Potassium Currents. Tests were performed on the voltage-dependent Kv1.1 and Kv1.2 channels expressed in *Xenopus* oocytes. The three drugs applied at 10 μM had a slight depressing effect on the three potassium currents (mean block: 12 ± 4%, n = 18), with the most effective compound in this respect being (*R*,*S*)-TMB (23 ± 6% current block; Fig. 4B). (*S*)-nor-TMB was the less active derivative (4 ± 3% block). This effect occurred without obvious changes in the cell resting potential and input resistance.

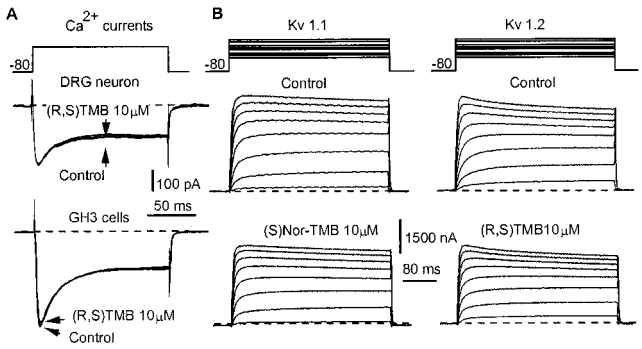

Fig. 4. Effect of TMB on voltage-dependent calcium and potassium currents. A, calcium currents from DRG neurons and GH_3 cells. Currents induced by 150-ms depolarization from −80 to −10 mV. B, potassium currents expressed in *Xenopus* oocytes. Superimposed current traces induced by 400-ms depolarizations at −40 to +20 mV (in 10-mV steps from −80 mV).

Rabbit Corneal Reflex

TMB produced a dose-dependent local anesthetic effect on rabbit cornea (Fig. 5A). The first significant effects were obtained using the 0.1% concentration and lasted 20 min. An instillation of 0.3% or 1% TMB produced a complete local anesthesia lasting more than 60 min. Under the same experimental conditions, lidocaine (Fig. 5) was found to be inactive up to the concentration of 0.3%. At the 6% concentration, the local anesthetic effect was complete only during 25 and 60 min after the instillation; there was no more inhibition of the corneal reflex. When comparing areas under the curve, we calculated that TMB showed a potency 17-fold higher than that of lidocaine.

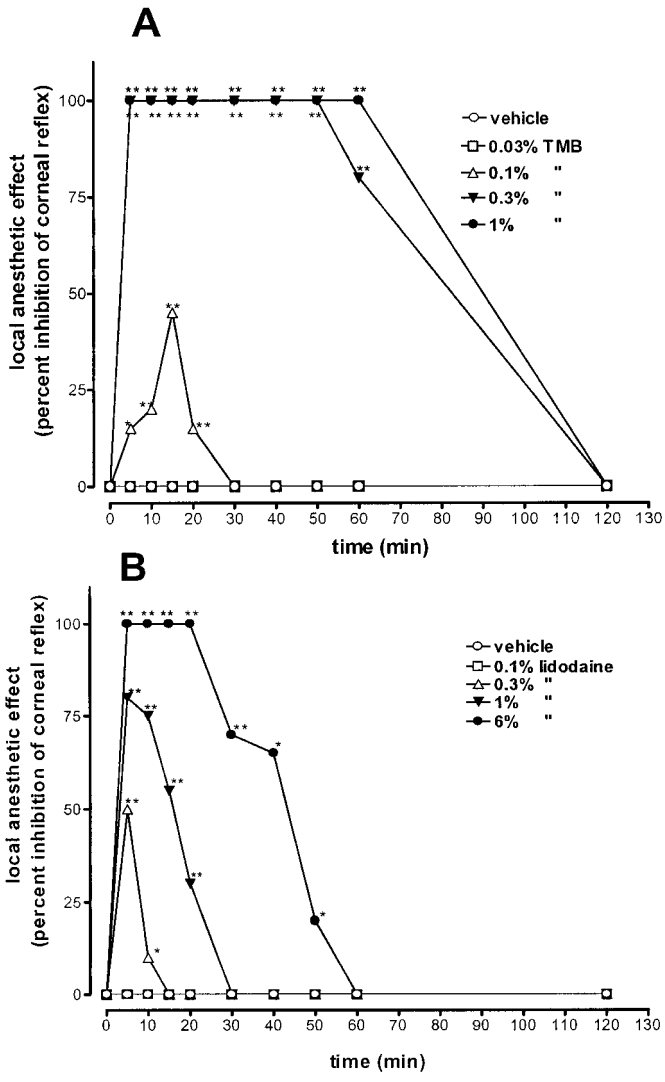

Fig. 5. Local anesthetic effect of TMB (A) and lidocaine (B) as determined in the rabbit corneal reflex. The values represent the median of percentage of inhibition of corneal reflex calculated for each set of 10 stimulations. The x-axis represents time (in minutes) after instillations. *$P < .05$; **$P < .01$ compared with the control group treated with the vehicle (Mann-Whitney U test).

Discussion

Our study shows that TMB, nor-TMB, and their corresponding stereoisomers inhibit veratridine-induced glutamate release in vitro. The lack of effect of morphine in this model suggests that the effects of TMB and nor-TMB on glutamate release are not due to the opioid properties of the compounds demonstrated in previous studies (Roman et al., 1987). The higher activity of nor-TMB (IC_{50} = 8.4 μM) compared with TMB (IC_{50} > 100 μM) is consistent with the reported affinity of these compounds for [^{3}H]batrachotoxin-binding sites. (*S*)-nor-TMB is the most active compound among the various tested compounds of the family, and such a result could not be expected from binding data. It is possible that the conditions we used in binding experiments do not allow a demonstration of the receptor-site stereospecificity. This may be different under the conditions used for superfusion, where ion concentrations may be able to better take stereospecificity into account. This phenomenon has been discussed by Triggle (1997). Stereospecificity of the drug action for ion channels may be directed by state-dependent interactions: in the case of sodium channels, for example, local anesthetic agents exhibit increasing stereoselectivity of action with decreasing membrane potential consistent with differences in the local anesthetic binding site geometry in different channel conformations. Lidocaine exhibits K_D values of 4×10^{-4} and 10^{-5} M for the resting and inactivated states of the sodium channels (Bean et al., 1983). In the case of drugs acting at calcium channels, similar observations have been made: nitrendipine exhibits an almost 1000-fold difference in affinity between the resting and inactivated states of the cardiac calcium channels (Sanguinetti and Kass, 1984). In our hands, bupivacaine displayed a potent inhibitory effect on veratridine-induced glutamate release, which may be related to its blocking properties on sodium channels. Veratridine is known to induce glutamate release by activating voltage-dependent sodium channels, resulting in sodium influx with consecutive reduction of the transmembrane gradient (Wermelskirchen et al., 1992). In agreement with our results, others have reported that compounds that inactivate voltage-dependent sodium channels prevent veratridine-induced glutamate release in vitro and in vivo (Lees and Leach, 1993). In a similar manner, the effect of TMB and related compounds on veratridine-induced glutamate release is probably due to their blocking activities on sodium channels.

Results on [^{3}H]batrachotoxin binding and glutamate release were confirmed by the electrophysiological data demonstrating that TMB, nor-TMB, and (*S*)-nor-TMB reversibly block the sodium currents in DRG neurons and in GH3 cells with almost the same efficiency ($IC_{50} \sim 1$ μM). Because the Hill coefficient is about 1, the blockade appeared to occur according to a simple bimolecular reaction (i.e., one molecule of blocker interacting with one site on the sodium channel). Therefore, the IC_{50} value measured the dissociation constant K_D of the blockers.

No effect could be demonstrated on calcium currents measured in GH3 cells and DRG neurons when using these compounds, and this result is different from that reported for TMB in other preparations. For example, the group of Nagasaki et al. (1993a), who worked on ileal smooth muscle cells, demonstrated that TMB reduced the calcium current in a concentration-dependent manner. The IC_{50} values were 5 and 36 μM after a holding potential of −40 and −60 mV, respectively. The slight depressing effect found for TMB on potassium currents was in agreement with results reported in ileal smooth muscle cells (Nagasaki et al., 1993b). In this work, it was shown that TMB inhibited an outward current consisting of a calcium-dependent potassium current (I_{KCa}) and a calcium-independent potassium current (I_{kv}). Taken together, the most potent effects of TMB were found on sodium channels in neuronal or GH3 cells with IC_{50} values of less than 1 μM, with the effects on Ca^{++} or potassium currents being observed at 10- to 100-fold higher concentrations.

The sodium channel-blocking activity was finally confirmed by the potent local anesthetic effect of TMB, which was 17-fold more active than lidocaine in terms of both potency and duration of action. Local anesthetic agents are known to block the generation and conduction of nerve impulses by inhibiting the current through voltage-gated sodium channels in the nerve cell membrane (Strichartz and Ritchie, 1987). The effect of TMB and related compounds on sodium currents, which is probably responsible for the inhibitory effect on glutamate release, indicates a potential therapeutic effect of these compounds in pain. Excitatory amino acids play an important role in the transmission of nociceptive message, and particularly in hyperalgesic conditions (Coderre et al., 1992). When a C-fiber containing both glutamate and substance P (Battaglia and Rustioni, 1988) is stimulated continuously with a sufficient frequency and intensity, the combined action of glutamate and neurokinins leads to removal of the NMDA channel block through a slow summating depolarization of the neuronal membrane (Urban et al., 1994). Once the channel is open, a massive depolarization of the neuron results from the fluxes of calcium into the cell. This causes a delayed sudden increase in activity called wind-up (Dickenson, 1995). The resultant amplification and prolongation of the response seem to underlie many forms of central hyperalgesia (Dray et al., 1994).

The role of the NMDA receptor in animal models of neuropathic pain and allodynia has been demonstrated by using NMDA antagonists: ketamine and dextromethorphan, for example, have been used successfully to treat opioid-insensitive neuropathies and cancer pains in humans (Mao et al., 1993). In this context, the therapeutic application of NMDA receptor antagonists for the treatment of chronic pain has been considered to be the most promising nonopioid-based approach. However, as in the case of neuroprotection, the delineation between spinal wind-up inhibition of nociceptive responses and unwanted behavioral effects appears to be a difficult challenge when using this class of drugs. In this context, the targeting of NMDA receptor subtypes may be a possibility for reaching greater safety margins. Another strategy consisting of the design of glutamate release inhibitors has been considered more promising than using excitatory amino acid receptor blockade in view of the multiple receptors and receptor target sites for glutamate. In this respect, glutamate release inhibition represents an exciting property of TMB in the perspective of its therapeutic use as analgesic agent.

Furthermore, clinical and animal studies have shown that concomitant opiate and local anesthetic therapy improves the magnitude and duration of pain relief compared with the effects of each drug administered separately (Meert and Melis, 1992). Because TMB and nor-TMB display micromolar affinities for μ and κ opioid receptors (Roman et al., 1987),

the association of this weak opioid property with sodium channel blockade and local anesthetic properties can explain the effectiveness of TMB in the therapy of abdominal pain. Another possibility is that the efficacy of TMB reported in patients with IBS could be due to the dual activity on abdominal pain and on bowel transit disturbances. These two approaches consisting of the treatment of pain together with the normalization of intestinal transit are generally recognized as able to produce improvement of symptoms in IBS patients. The intestinal regulatory role of TMB has been demonstrated in studies where the rate of colonic motor activity returned to normal under TMB in patients with either a hyperkinetic or a hypokinetic colon (Meunier, 1980; Reboa et al., 1976). TMB increased the number of long spike bursts in constipated patients (Frexinos et al., 1985), whereas it decreased this number in patients with diarrhea-predominant IBS (Schang et al., 1993).

On the other hand, an enhancement of visceral perception has been demonstrated in patients with functional digestive disorders, and particularly in patients with IBS. In these patients, the colonic threshold of pain perception is lowered compared with control subjects (Bradette et al., 1994). Recently, it has been shown in an animal study that TMB may influence the activity of visceral afferents (Julia et al., 1996). In conscious rats as well as in humans, rectal distention induces a rectocolonic reflex characterized by an inhibition of colonic motility after rectal distention. In this model, TMB significantly decreased the intensity of this inhibitory effect at a dose of 5 mg/kg i.p. The blocking effect of TMB on sodium channel currents may account for this antinociceptive effect.

In humans, the major circulating compound after TMB oral administration is nor-TMB, which has similar or more potent effects than TMB itself on sodium channel blockade and glutamate release inhibition. This compound may be responsible for the efficacy found in patients with IBS in attacks of abdominal pain (Lüttecke, 1980, Toussaint et al., 1981, Ghidini et al., 1986).

The biochemical and pharmacological data reported in this study allow a better understanding of the mechanism of action of TMB. They support the assumption that besides its regulatory effects on colonic motility, which have been reported in the past and which had been related to its weak opioid properties, TMB is endowed with antinociceptive properties that could be due to its blocking effect on sodium channels. These unique properties of TMB explain how this compound may demonstrate a much improved therapeutic potential in humans than that expected from a simple spasmolytic compound.

References

Allescher HD, Ahmad S, Classen M and Daniel EE (1991) Interaction of trimebutine and JO-1196 (fedotozine) with opioid receptors in the canine ileum. *J Pharmacol Exp Ther* **257:**836–842.

Battaglia G and Rustioni A (1988) Coexistence of glutamate and substance P in dorsal root ganglion cells of the rat and monkey. *J Comp Neurol* **27:**302–312.

Bean BP, Cohen CJ and Tsien RW (1983) Lidocaine block of cardiac sodium channels. *J Gen Physiol* **81:**613–642.

Bourget P and Delouis JM (1993) Review of a technic for the estimation of area under the concentration curve in pharmacokinetic analysis. *Therapie* **48:**1–5.

Bradette M, Delvaux M, Staumont G, Fioramonti G, Bueno L and Frexinos J (1994) Evaluation of colonic sensory thresholds in IBS patients using a barostat: Definition of optimal conditions and comparison with healthy subjects. *Dig Dis Sci* **39:**449–457.

Bueno L, Honde C, Pascaud X and Junien JL (1987) Effects of orally versus parenterally administrated trimebutine on gastrointestinal and colonic motility in dogs. *Gastroenterol Clin Biol* **11:**90B–93B.

Cheng YC and Prusoff WH (1973) Relationship between the inhibition constant (K_i) and the concentration of inhibitor which causes 50 percent inhibition (IC_{50}) of an enzymatic reaction. *Biochem Pharmacol* **22:**3099–4002.

Coderre TJ and Melzack R (1992) The contribution of excitatory amino acids to central sensitization and persistent nociception after formalin-induced tissue injury. *J Neurosci* **12:**3665–3670.

Delis C, Walker EA, Castillo FD, Evans DF, Wingate DL, Allouche S and Van Egroo LD (1994) The effect of stress and opioid agonist on postprandial motor activity in the human small bowel (Abstract). *Gastroenterology* **106:**A485.

Dickenson AH (1995) Spinal cord pharmacology of pain. *Br J Anesth* **75:**193–200.

Dray A, Urban L and Dickenson A (1994) Pharmacology of chronic pain. *Trends Pharmacol Sci* **15:**190–197.

Frexinos J, Fioramonti J and Bueno L (1985) Effect of trimebutine on colonic myoelectrical activity in IBS patients. *Eur J Clin Pharmacol* **28:**181–185.

Ghidini O, Saponati G and Intrieri L (1986) Single drug treatment for irritable colon: Rociverine versus trimebutine maleate. *Curr Ther Res* **39:**541–548.

Grandjouan S, Chaussade S, Couturier D, Thierman-Duffaud D and Henry JF (1989) A comparison of metoclopramide and trimebutine on small bowel motility in humans. *Aliment Pharmacol Ther* **3:**387–393.

Julia V, Coelho AM, Rouzade MI, Allouche S and Bueno L (1996) Influence de la trimébutine (Débridat) sur l'hypomotricité colique et les crampes abdominales liées á la distension rectale chez le rat. *Med Chir Dig* **25:**239–242.

Lees G and Leach MJ (1993) Studies on the mechanism of action of the novel anticonvulsant lamotrigine (Lamictal) using primary neuroglial cultures from rat cortex. *Brain Res* **612:**190–199.

Lüttecke K (1980) A three part controlled study of trimebutine in the treatment of irritable colon syndrome. *Curr Med Res Opin* **6:**437–443.

Mao J, Price DD, Hayes RL, Lu J, Mayer DJ and Frenk H (1993) Intrathecal treatment with dextrorphan or ketamine potently reduces pain-related behaviors in a rat model of peripheral mononeuropathy. *Brain Res* **605:**164–168.

Matesson DR and Armstrong CM (1984) Na and Ca channels in a transformed line of anterior pituitary cells. *J Gen Physiol* **83:**371–394.

McPherson GA (1985) Analysis of radioligand binding experiments: A collection of computer programs for the IBM PC. *J Pharmacol Methods* **14:**213–228.

Meert TF and Melis W (1992) Interactions between epidurally and intrathecally administered sufentanil and bupivacaine in hydroxypropyl-β-cyclodextrin in the rat. *Acta Anesthesiol Belg* **43:**79–89.

Meunier P (1980) Effet de la trimébutine sur la motricité colique dans les colopathies (Abstract). *Gastroenterol Clin Biol* **4:**261A.

Moshal MG and Herron M (1979) A clinical trial of trimebutine in spastic colon. *J Int Med Res* **7:**231–234.

Nagasaki M, Komori S and Ohashi H (1993a) Effect of trimebutine on voltage-activated calcium current in rabbit ileal smooth muscle cells. *Br J Pharmacol* **110:**399–403.

Nagasaki M, Komori S, Tamaki H and Ohashi H (1993b) Effect of trimebutine on K^+ current in rabbit ileal smooth muscle cells. *Eur J Pharmacol* **235:**197–203.

Pascaud X, Roman F, Petoux F, Vauche D and Junien JL (1987) Action de la trimebutine sur la motricité gastro-intestinale. *Gastroenterol Clin Biol* **11:**77B–81B.

Reboa G, Bertoglio C, Terrizzi A and Parodi E (1976) L'azione della trimebutina sull'attivita elettrica e manometrica del colon normale e patologico. *Riv Gastroenterol* **28:**1–16.

Roman F, Pascaud X, Taylor JE and Junien JL (1987) Interactions of trimebutine with guinea pig opioid receptors. *J Pharm Pharmacol* **39:**404–407.

Sanguinetti MC and Kass RS (1984) Voltage-dependent block of calcium channel current in the calf cardiac Purkinje fiber by dihydropyridine calcium channel antagonists. *Circ Res* **55:**336–348.

Schang JC, Devroede G and Pilote M (1993) Effect of trimebutine on colonic function in patients with chronic idiopathic constipation: Evidence for the need of a physiologic rather than clinical selection. *Dis Colon Rectum* **36:**330–336.

Strichartz G and Ritchie J (1987) The action of local anesthetics on ion channels of excitable tissues, in *Local Anesthetics Handbook of Experimental Pharmacology* (Strichartz G ed) pp 21–52, Springer-Verlag, Heidelberg.

Toussaint J, Cremer M and Pintens H (1981) Etude en simple aveugle de trimébutine et de la mébévérine dans le côlon irritable et la dyspepsie. *Acta Ther* **7:**261–268.

Triggle DJ (1997) Stereoselectivity of drug action (Review). *Drug Discovery Today* **2:**138–147.

Turner TJ and Dunlap K (1995) Prolonged time course of glutamate release from nerve terminals: Relationship between stimulus duration and the secretory event. *J Neurochem* **64:**2022–2033.

Urban L, Thompson SWN and Dray A (1994) Modulation of spinal excitability: Co-operation between neurokinin and excitatory amino acid neurotransmitters. *Trends Neurosci* **17:**432–438.

Valmier J, Simmoneau M and Boisseau S (1989) Expression of voltage-dependent sodium and transient potassium currents in an identified subpopulation of dorsal root ganglion cells acutely isolated from 12-day-old mouse embryos. *Pfluegers Arch* **414:**360–368.

Wang H, Kunkel DD, Schwartzkroin PA and Tempel BL (1994) Localization of Kv1.1 and Kv1.2, two K channel proteins, to synaptic terminals, somata, and dendrites in the mouse brain. *J Neurosci* **14:**4588–4599.

Wermelskirchen D, Wilffert B and Peters TJ (1992) Veratridine-induced intoxication: An in vitro model for the characterization of anti-ischemic compounds. *Basic Clin Physiol Pharmacol* **3:**293–321.

Send reprint requests to: Dr. François J. Roman, Institut de Recherche Jouveinal/Parke-Davis, 11-13, rue de la Loge, BP 100, 94263 Fresnes Cedex, France. E-mail: francois.roman@wl.com